

Immune pathway upregulation and lower genomic instability distinguish EBV-positive nodal T/NK-cell lymphoma from ENKTL and PTCL-NOS

Cho Mar Myint Wai,^{1*} Shangying Chen,^{2*} The Phyu,¹ Shuangyi Fan,¹ Sai Mun Leong,¹ Wenning Zheng,³ Louis Ching Yi Low,¹ Shoa-Nian Choo,¹ Chi-Kuen Lee,¹ Tae-Hoon Chung,³ Kenneth Hon Kim Ban,² Soumita Ghosh,³ Stefanus Lie,³ Seiichi Kato,^{4,5} Shigeo Nakamura,⁴ Emiko Takahashi,⁶ Young-Hyeh Ko,⁷ Joseph D. Khoury,⁸ Shih-Sung Chuang,⁹ Rex K.H. Au-Yeung,¹⁰ Soo-Yong Tan,¹¹ Soon-Thye Lim,¹² Choon-Kiat Ong,¹³⁻¹⁵ Yong-Howe Ho,¹⁶ Li Mei Poon,¹⁷ Sanjay de Mel,¹⁷ Anand D. Jeyasekharan,³ Wee-Joo Chng,^{3,17,18} Franziska Otto,¹⁹ Leticia Quintanilla-Martinez,¹⁹ Federica Zanardi,²⁰ Fabio Iannelli,²⁰ Claudio Tripodo,²¹ Jason J. Pitt³ and Siok-Bian Ng^{1,3,11}

¹Department of Pathology, Yong Loo Lin School of Medicine, National University of Singapore, Singapore; ²Department of Biochemistry, Yong Loo Lin School of Medicine, National University of Singapore, Singapore; ³Cancer Science Institute of Singapore, National University of Singapore, Singapore; ⁴Department of Pathology and Laboratory Medicine, Nagoya University Hospital, Nagoya, Japan; ⁵Department of Pathology and Molecular Diagnostics, Aichi Cancer Center Hospital, Nagoya, Japan; ⁶Department of Pathology, Aichi Medical University Hospital, Nagakute, Japan; ⁷Department of Pathology, Samsung Medical Center, Sungkyunkwan University, Seoul, Korea; ⁸Department of Hematopathology, The University of Texas MD Anderson Cancer Center, Houston, TX, USA; ⁹Department of Pathology, Chi-Mei Medical Center, Tainan, Taiwan; ¹⁰Department of Pathology, Queen Mary Hospital, The University of Hong Kong, Hong Kong SAR, China; ¹¹Department of Pathology, National University Hospital, National University Health System, Singapore; ¹²Lymphoma Genomic Translational Research Laboratory, National Cancer Center Singapore, Singapore; ¹³Division of Medical Oncology, National Cancer Center Singapore, Singapore; ¹⁴Lymphoma Genomic Translational Research Laboratory, Division of Medical Oncology, National Cancer Centre Singapore, Singapore; ¹⁵Duke-NUS Medical School, Singapore; ¹⁶Genome Institute of Singapore, A*STAR (Agency for Science, Technology and Research), Singapore; ¹⁷Department of Pathology, Tan Tock Seng Hospital, Singapore; ¹⁸Department of Hematology-Oncology, National University Cancer Institute Singapore, National University Hospital, National University Health System, Singapore; ¹⁹Department of Medicine, Yong Loo Lin School of Medicine, National University of Singapore, Singapore; ²⁰Institute of Pathology and Neuropathology, Eberhard Karls University of Tübingen and Comprehensive Cancer Center, Tübingen University Hospital, Tübingen, Germany; ²¹Bioinformatics Unit, IFOM - the FIRC Institute of Molecular Oncology, Milan, Italy and ²¹Tumor Immunology Unit, University of Palermo School of Medicine, Palermo, Italy

*CMMW and SC contributed equally as co-first authors.

Abstract

Primary Epstein-Barr virus (EBV)-positive nodal T/NK-cell lymphoma (PTCL-EBV) is a poorly understood disease which shows features resembling extranodal NK/T-cell lymphoma (ENKTL) and is currently not recognized as a distinct entity but categorized as a variant of primary T-cell lymphoma not otherwise specified (PTCL-NOS). Herein, we analyzed copy-number aberrations (n=77) with a focus on global measures of genomic instability and homologous recombination deficiency and performed gene expression (n=84) and EBV miRNA expression (n=24) profiling as well as targeted mutational analysis (n=16) to further characterize PTCL-EBV in relation to ENKTL and PTCL-NOS. Multivariate analysis revealed that patients with PTCL-EBV had a significantly worse outcome compared to patients with PTCL-NOS ($P=0.002$) but not to those with ENKTL. Remarkably, PTCL-EBV exhibited significantly lower genomic instability and homologous recombination deficiency scores compared to ENKTL and PTCL-NOS. Gene set enrichment analysis revealed that many immune-related pathways, interferon α/γ response, and IL6_JAK_STAT3 signaling were significantly upregulated in PTCL-EBV and correlated with lower genomic instability scores. We also identified that NF κ B-associated genes, *BIRC3*, *NFKB1* (*P50*) and *CD27*, and their proteins are upregulated in PTCL-EBV. Most PTCL-EBV demonstrated a type 2 EBV latency pattern and, strikingly, exhibited downregulated expression of most EBV miRNA compared to ENKTL and their target

Correspondence:

Siok-Bian Ng (lead contact)
patnsb@nus.edu.sg

Jason J. Pitt
jason.j.pitt@nus.edu.sg

Received: September 9, 2021.


Accepted: January 4, 2022.

Prepublished: January 13, 2022.

<https://doi.org/10.3324/haematol.2021.280003>

©2022 Ferrata Storti Foundation

Haematologica material is published under

a CC-BY-NC license 

genes were also enriched in immune-related pathways. PTCL-EBV also showed frequent mutations of TET2, PIK3CD and STAT3, and are characterized by microsatellite stability. Overall, poor outcome, low genomic instability, upregulation of immune pathways and downregulation of EBV miRNA are distinctive features of PTCL-EBV. Our data support the concept that PTCL-EBV could be considered as a distinct entity, provide novel insights into the pathogenesis of the disease and offer potential new therapeutic targets for this tumor.

Introduction

Primary nodal Epstein-Barr virus (EBV)-positive T/NK-cell lymphoma is an uncommon group of peripheral T-cell lymphomas (PTCL) that presents primarily with lymph node disease but may involve a limited number of extranodal organs.¹ While the majority of PTCL-EBV are derived from T cells, a minority are *bona fide* NK-cell lymphomas. They show significant overlap with extranodal NK/T-cell lymphoma, nasal type (ENKTL) as both tumors are associated with EBV and characterized by cytotoxic T- or NK-cell proliferation. EBV-positive nodal T/NK-cell lymphomas are more common in the elderly, usually demonstrate a monomorphic growth pattern and lack angiodestruction and prominent necrosis.^{2,3} A few reports have described clinicopathological features distinct from those of ENKTL, including the lack of nasal involvement, frequent T-cell origin, and a CD8⁺/CD56⁻ phenotype.^{2,4}

The 2017 World Health Organization (WHO) lymphoma classification recommends that EBV-positive nodal T/NK-cell lymphoma be considered as an EBV-positive variant of PTCL, not otherwise specified (PTCL-NOS) as data on this disease are limited, and it is currently unclear whether this group of lymphomas represents a distinct entity.⁵ The molecular biology of EBV-positive nodal T/NK-cell lymphoma, henceforth referred to as an EBV-positive variant of PTCL (PTCL-EBV), and its relationship with ENKTL and PTCL-NOS remains poorly understood - mainly due to the rarity of these tumors and lack of tissue availability.

Genomic instability (GI) is a hallmark of cancer and refers to the propensity of cells to accumulate a variety of DNA alterations. These alterations, a subset of which provides a selective growth advantage instrumental for tumorigenesis and progression, may delineate different profiles in entities sharing phenotypic or transcriptional features.⁶ Importantly, the broad characteristics of GI, as measured by scores, have prognostic and management implications, specifically with regard to the choice of therapeutic agents.⁷

Given the rarity of PTCL-EBV, scarcity of frozen samples and lack of available cell lines, we leveraged formalin-fixed paraffin-embedded tissues. Using gene expression profiling and testing of copy number aberrations, we previously compared PTCL-EBV to ENKTL and showed that PTCL-EBV is characterized by PD-L1 upregulation, expression of T-cell related genes and frequent loss of

14q11.2, which correlates with loss of TCRA loci and T-cell origin.^{4,8} For the current study, we expanded the disease types and included PTCL-NOS in the comparison, and performed a comprehensive suite of analyses including EBV miRNA expression, custom gene panel sequencing and copy number aberration analysis focusing on global measures of GI. We further re-profiled the gene expression signatures using an improved microarray on our cases, including those studied in the previous work.⁴ Interestingly, we demonstrated that PTCL-EBV displays a remarkably lower degree of GI despite its more aggressive outcome among the three diseases and is characterized by upregulation of immune-related pathways and lower expression of EBV miRNA compared to ENKTL and PTCL-NOS. These novel findings not only offer insights into the pathogenesis of PTCL-EBV and raise considerations regarding its treatment, but also support the proposal that PTCL-EBV is a distinct entity in the WHO classification.

Methods

Study cohort

Cases from multiple institutions were reviewed by two hematopathologists to confirm the diagnosis of ENKTL (n=89), PTCL-EBV (n=25) and PTCL-NOS (n=36) based on the 2017 WHO lymphoma classification.⁵ PTCL-EBV shows a similar phenotype as ENKTL but, unlike ENKTL, (i) patients present primarily with nodal disease where the bulk of tumor is localized; (ii) nasal involvement is lacking; (iii) it often shows a CD8⁺/CD56⁻ phenotype; and (iv) it is often of T-cell origin (*Online Supplementary Table S1*). Systemic and cutaneous EBV-positive T/NK lymphoproliferative diseases occurring in children were excluded. The diagnosis of PTCL-NOS was established when other specific subtypes of PTCL had been excluded. Cytotoxicity was defined as the expression of at least one cytotoxic marker (TIA1, granzyme B). Clinical data including age, sex, disease type, stage, International Prognostic Index (IPI) score, expression of CD4, CD8 and CD56, T or NK lineage, treatment and overall survival were obtained (*Online Supplementary Table S2A, B*). This study was approved by the National Healthcare Group Domain Specific Review Board B (2009/00212).

Copy number aberration analysis

An OncoScan® FFPE assay was performed on 34 ENKTL,

14 PTCL-EBV and 29 PTCL-NOS cases as previously published.⁹ Copy number aberrations were analyzed using OncoScan[®] Console (v1.3) software (ThermoFisher Scientific, Waltham, MA, USA). Segmentation results were analyzed using GISTIC (v2.0.22)¹⁰ with the GENCODE hg19 build. GI and homologous recombination deficiency (HRD) scores were calculated according to published methods.¹¹

Gene expression profiling

Gene expression profiling was performed on 35 ENKTL, 23 PTCL-EBV, and 26 PTCL-NOS cases using a GeneChip[®] Clariom D Assay (Human) array and the data were analyzed as described previously.¹² Gene expression profiling (GSE160119) and copy number aberration (GSE160118) raw data were deposited in the Gene Expression Omnibus (GEO).

Polymerase chain reaction analysis of EBV miRNA and EBV latency

Quantitative reverse transcription polymerase chain reaction (RT-qPCR) analysis of miRNA expression was performed using IDEAL miRNA qPCR assays (MiRXES, Singapore) (n=24) according to the manufacturer's instructions on a QuantStudio[™] 5 System (ThermoFisher Scientific, Waltham, MA, USA). RT-qPCR of EBV genes was performed to confirm EBV latency in PTCL-EBV and ENKTL.

Fluorescence *in situ* hybridization and multiplex immunofluorescence

Fluorescence *in situ* hybridization (FISH), multiplex immunofluorescence and multispectral imaging were performed as previously described.⁴

Mutational analysis targeted next-generation sequencing

Targeted mutation analysis was performed by next-generation sequencing (Ion GeneStudio S5 prime, Thermo Fisher Scientific, Waltham, MA, USA) using an AmpliSeq customized T/NK-lymphoid panel comprising 35 genes recurrently mutated in ENKTL and PTCL-NOS (*Online Supplementary Table S3A*) and the 484-gene NovoPMTM 2.0 panel (*Online Supplementary Table S3B*) (total 500 genes including 19 common genes).

Statistical methods

Overall survival was investigated using Kaplan-Meier non-parametric survival analysis and log-rank tests. The effects of disease type, age, sex and disease stage were analyzed using unadjusted univariate and multivariate Cox proportional hazard models. Analyses were performed in R with the "survival" (v0.1.2) and "survminer" (v0.4.6) packages. Gene expression profiling analysis was performed in R with the "limma" package (v3.40.6). Unsupervised hier-

archical clustering was performed using Spearman distance and Ward.D2 linkage. All additional statistical tests were performed in R.

The diagnostic criteria for the diseases, T/NK lineage assignment, detailed descriptions of study cohorts, experimental methods, data analysis and data accession are provided in the *Online Supplementary Materials*.

Results

Differences in clinical and survival variables among the disease groups

The salient clinicopathological and immunohistochemical features of ENKTL, PTCL-EBV and PTCL-NOS are summarized in Table 1A and *Online Supplementary Table S2A, B*. All 25 patients with PTCL-EBV, comprising 14 Japanese, eight Chinese, two Korean and one Bangladeshi person, presented with nodal disease and the bulk of disease involved lymph nodes. Phenotypically, PTCL-EBV was often positive for CD8 (17/25, 68%), cytotoxic markers (100%) and TCRB (12/25, 48%). CD56 was commonly negative (18/24, 75%) and none of the cases tested expressed TCRG. Four of 23 (17%) cases tested expressed CD4, of which one was positive for CXCL13 and CD10 (focal). Most of the cases of PTCL-EBV were of T-cell origin (20/23, 87%), in accordance with previous reports^{3,13-15} (Figure 1A). With regards to treatment, the patients in all three groups from different institutions were treated with a heterogeneous combination of chemotherapy regimens (*Online Supplementary Table S2A*). This is understandable as these are rare lymphomas lacking standardized and effective treatment. Two out of 15 PTCL-EBV patients with known treatment data were treated with SMILE therapy. One died 3.5 months after diagnosis and the other died 12.6 months after diagnosis.

Despite the treatment heterogeneity, our results revealed that patients with PTCL-EBV had a significantly shorter median overall survival (4.6 months) compared to those with ENKTL (14.7 months, $P=0.001$) and PTCL-NOS (26 months, $P=0.007$). (Figure 1B; Table 1). Univariate analysis identified advanced disease stage (stage 4) ($P<0.001$) and older age ($P=0.001$) as significantly associated with poor prognosis. Compared to patients with PTCL-EBV, patients with ENKTL had a 61% lower risk of death (HR=0.39, 95% CI: 0.22-0.69, $P=0.001$), while those with PTCL-NOS had a 59% lower risk (HR=0.41, 95% CI: 0.21-0.80, $P=0.009$). After adjusting for disease stage, sex and age, PTCL-NOS remained significantly less aggressive compared to PTCL-EBV (HR=0.3, 95% CI: 0.14-0.65, $P=0.002$) (Table 2). A Cox proportional-hazards model was also performed and after controlling for lineage, patients with PTCL-EBV showed significantly worse outcome than those with ENKTL (HR=2.34, 95% CI: 1.05-5.24, $P=0.038$), indicating that the

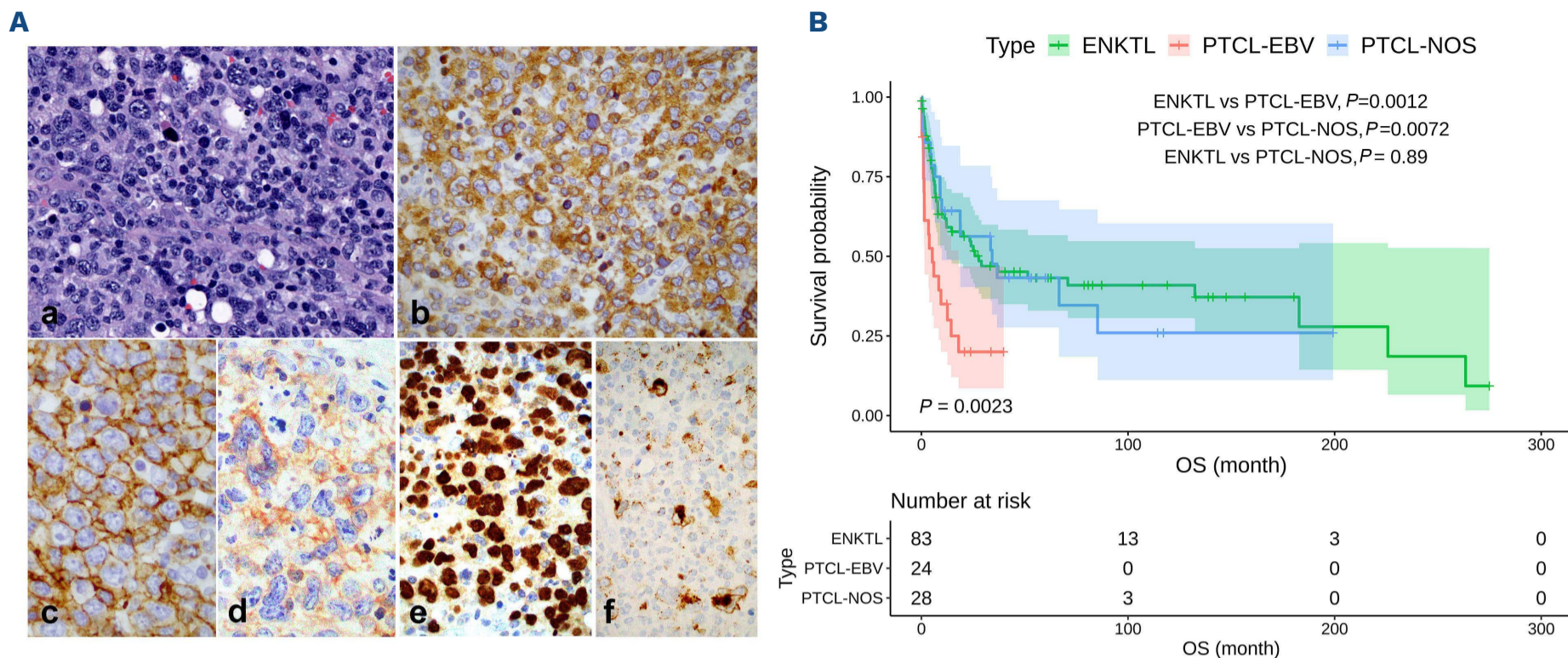


Figure 1. Morphological features and survival of PTCL-EBV patients compared to those with ENKTL and PTCL-NOS. (A) Representative images of PTCL-EBV. The tumor cells are large and pleomorphic (a, Hematoxylin & eosin, original magnification x400). They are positive for CD3 (b, original magnification x400), CD8 (c, original magnification x600), T-cell receptor, beta (TCR β) (d, original magnification x600), EBER (e, original magnification x400) and granzyme B (f, original magnification x400). The positive expression for TCR β indicates a T-cell origin. (B) Kaplan-Meier survival curve depicting overall survival of three disease groups. Patients in the PTCL-EBV group had significantly shorter overall survival compared to those in the ENKTL and PTCL-NOS groups.

Table 1. Clinicopathological features and gene expression profiling in patients with ENKTL, PTCL-EBV and PTCL-NOS.

Parameters	ENKTL (N=89)	PTCL-EBV (N=25)	PTCL-NOS (N=36)	P
Median age in years (range, SD)	49 (17-82, 16.20)	59 (32-89, 14.43)	62 (11-95, 18.22)	0.002*
Female/male, N	27/62	5/20	13/23	0.399 [†]
COO, T/NK/indeterminate, N	16/57/16	20/3/2	36/0/0	<0.001 [†]
Stage [‡] , 1&2/3&4, N	52/29	3/20	4/22	<0.001 [†]
IPI score [‡] , low/intermediate/high, N	37/24/8	3/11/6	1/6/5	0.001 [†]
Median survival [‡] in months	14.7	4.6	26.0	0.002 [†]
CD56 [‡] positive/negative, N	66/20	6/18	1/25	<0.001 [†]
CD8 [‡] positive/negative, N	11/64	17/8	11/25	<0.001 [†]
TCR β [‡] positive/negative, N	9/51	12/13	12/6	<0.001 [†]
TCR γ [‡] positive/negative, N	2/54	0/14	6/12	0.002 [†]

*Kruskal-Wallis test, [†]chi-square test, [‡]only cases with available data were included for analysis, [§]log-rank test; SD: standard deviation; COO, cell of origin; IPI: International Prognostic Index.

Table 2. Univariate and multivariate analyses for overall survival in the ENKTL, PTCL-EBV and PTCL-NOS groups.

Variable	Category	Univariate			Multivariate		
		HR	CI (95%)	P	HR	CI (95%)	P
Disease type	ENKTL	0.39	0.22-0.69	0.001	0.65	0.34-1.26	0.2
	PTCL-EBV	1	Ref		1	Ref	
	PTCL-NOS	0.41	0.21-0.80	0.009	0.3	0.14-0.65	0.002
Stage	1	1	Ref		1	Ref	
	2	1.33	0.54-3.22	0.50	1.5	0.61-3.67	0.4
	3	2.46	1.00-6.07	0.051	1.56	0.51-4.81	0.4
	4	4.18	2.31-7.57	<0.001	4.56	2.43-8.54	<0.001
Sex	Female	1	Ref		1	Ref	
	Male	1.23	0.76-1.99	0.40	1.38	0.82-2.32	0.2
Age		1.02	1.01-1.04	0.001	1.02	1.01-1.04	0.006
IPI score	Low	1	Ref				
	Intermediate	5.16	2.32-11.5	<0.001			
	High	8.33	3.48-19.9	<0.001			

HR: hazard ratio; CI: confidence interval; Ref: reference; IPI: International Prognostic Index.

worse outcome of PTCL-EBV patients compared to ENKTL patients is independent of lineage. Interestingly, there was no longer a significant difference in the survival outcome between ENKTL and PTCL-EBV patients, suggesting that the worse outcome of those with PTCL-EBV could be ascribed to older age and more advanced disease stage at diagnosis.

Differences in focal copy number aberrations among disease groups

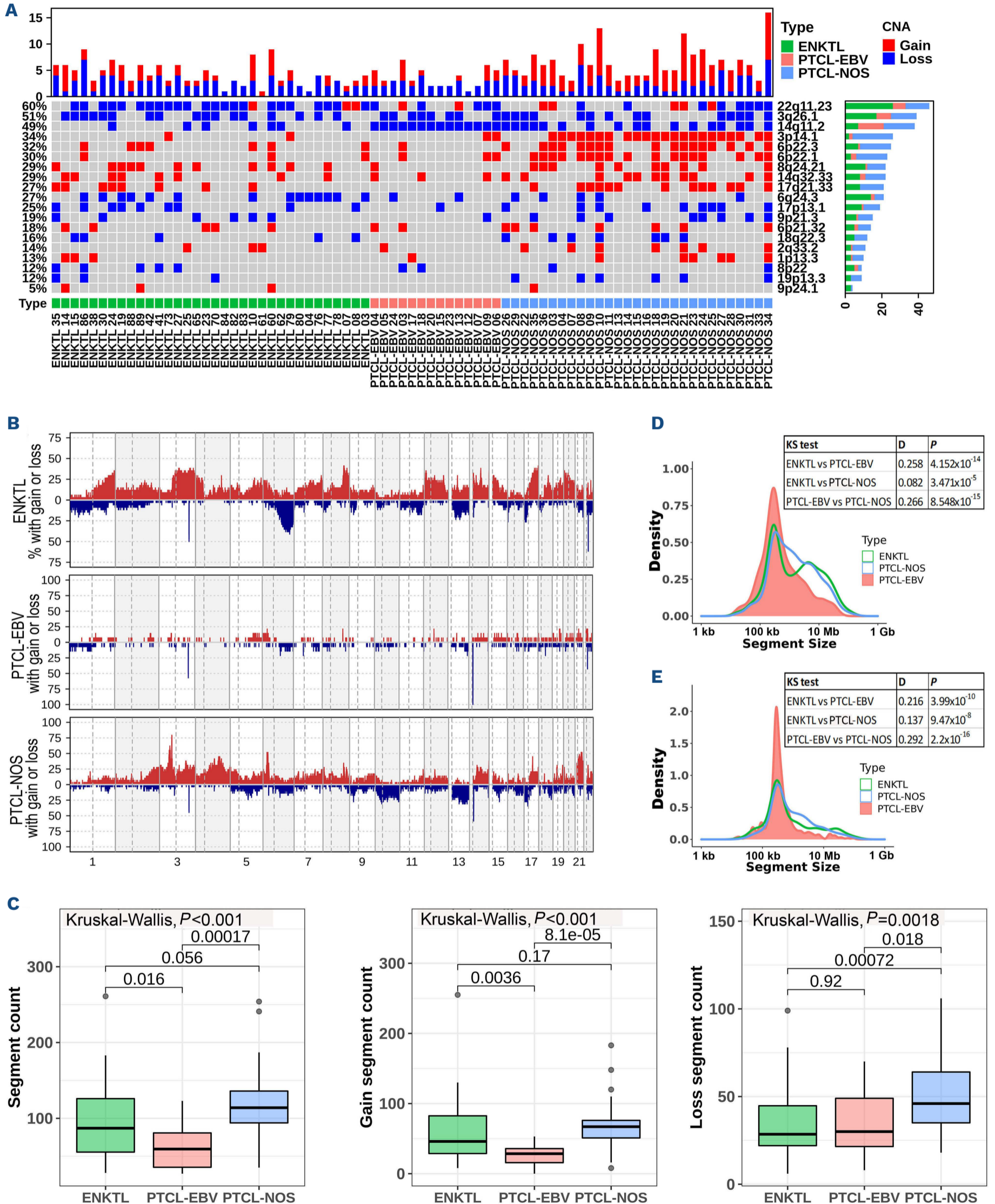
In order to identify differences in copy number profiles of the three diseases, we analyzed copy number aberrations of patients with ENKTL (n=34), PTCL-EBV (n=14) and PTCL-NOS (n=29) and identified recurrent aberrations (q<0.25) with their putative target genes across all samples (Figure 2A). Previously,⁴ comparing ENKTL (n=29) and PTCL-EBV (n=12), we noted differences in 14q11.2 and were able to reproduce those here. However, with the addition of five and two new ENKTL and PTCL-EBV samples, respectively – as well as a cohort of PTCL-NOS – we were able to identify multiple unreported differences in focal copy number aberration rates across these groups.

Of the 11 recurrently gained regions, 3p14.1, 6p22.3, 6p22.1 and 17q21.33 occurred at significantly different frequencies across disease groups ($P<0.05$, χ^2 test) (*Online Supplementary Table S4*). Gain of 3p14.1 was found in 14.3% of PTCL-EBV cases compared to 5.9% and 76.0% of ENKTL and PTCL-NOS cases, respectively ($P<0.001$). Gain of 6p22.3 was observed more frequently in ENKTL (20.6%) and PTCL-NOS (58.6%) than in PTCL-EBV (7.1%) ($P=0.005$). Gain of 6p22.1 was observed in 21.4% of PTCL-EBV cases compared to 8.8% of ENKTL and 58.6% of PTCL-NOS cases

($P=0.001$). Of the nine recurrent losses, only 14q11.2 occurred at significantly different frequencies among the disease groups (*Online Supplementary Table S5*). As expected, loss of 14q11.2 was observed in 100% of PTCL-EBV cases,⁴ whereas it was only found in 20.6% and 58.6% of ENKTL and PTCL-NOS, respectively ($P=0.001$). It is unclear whether the high frequency of 14q11.2 loss in PTCL-EBV is a result of additional critical driver events occurring at the TCRA locus, on top of monoclonal TCRA gene rearrangement, or related to preferential TCR usage in PTCL-EBV due to possible underlying immune perturbations and antigen selection that predispose to malignancy.¹⁶ The 14q11.2 loss in PTCL-NOS is slightly low, which may be a result of coverage bias related to the probe design of the Oncoscan assay or a lack of TCRA rearrangement in some PTCL-NOS cases.⁸ The top two recurrent copy-number gains (3p14.1 and 6p22.1) were subsequently validated by FISH (*Online Supplementary Figure S1* and *Online Supplementary Table S6*).

PTCL-EBV exhibits lower genomic complexity than other disease groups

We further compared the genome-wide levels of copy number aberrations across the three disease types (Figure 2B, *Online Supplementary Figure S2*). Analysis of copy number burden (segment counts) revealed that PTCL-EBV exhibited significantly fewer segments than ENKTL ($P=0.016$, Mann-Whitney U test) and PTCL-NOS ($P<0.001$) (Figure 2C, left panel). While copy number segment differences between ENKTL and PTCL-EBV appeared primarily driven by gains (Figure 2C, middle panel), PTCL-NOS demonstrated increased losses compared to other groups



Continued on following page.

Figure 2. Composite copy number alteration profiles of three disease groups. (A) Composite map showing the focal copy number alteration spectrum in three disease groups. The red and blue represent copy number gain and loss, respectively. Each row represents a genomic locus while each column represents a case. Bars on the right represent the proportion of each disease type in copy number aberrations identified. PTCL-EBV patients had fewer focal copy number aberrations compared to patients with ENKTL and PTCL-NOS. (B) Penetrance plots showing the frequency of gains and losses of genomic loci in ENKTL, PTCL-EBV and PTCL-NOS groups. The X-axis represents chromosome number and the Y-axis indicates the proportion of gain or loss of the corresponding genomic loci within the corresponding population. Red bars denote copy number gains and blue bars denote copy number losses. PTCL-EBV exhibited less frequent genomic alterations compared to other disease groups. (C) Boxplot depicting total copy number segment counts (left), gains only (middle) and losses only (right) across the three diseases. Differences among the three groups were determined using the Kruskal-Wallis test while pairwise comparisons were assessed by the Mann-Whitney U test (*P* values shown). PTCL-EBV displayed lower segment counts compared to ENKTL and PTCL-NOS. (D, E) Copy number segment size distribution of gains (D) and losses (E) in the three disease groups. Statistical significance was determined using a two-sample Kolmogorov-Smirnov test with *P* values indicated in the table. PTCL-EBV gain and loss distributions were enriched for smaller copy number segments compared to the other disease groups.

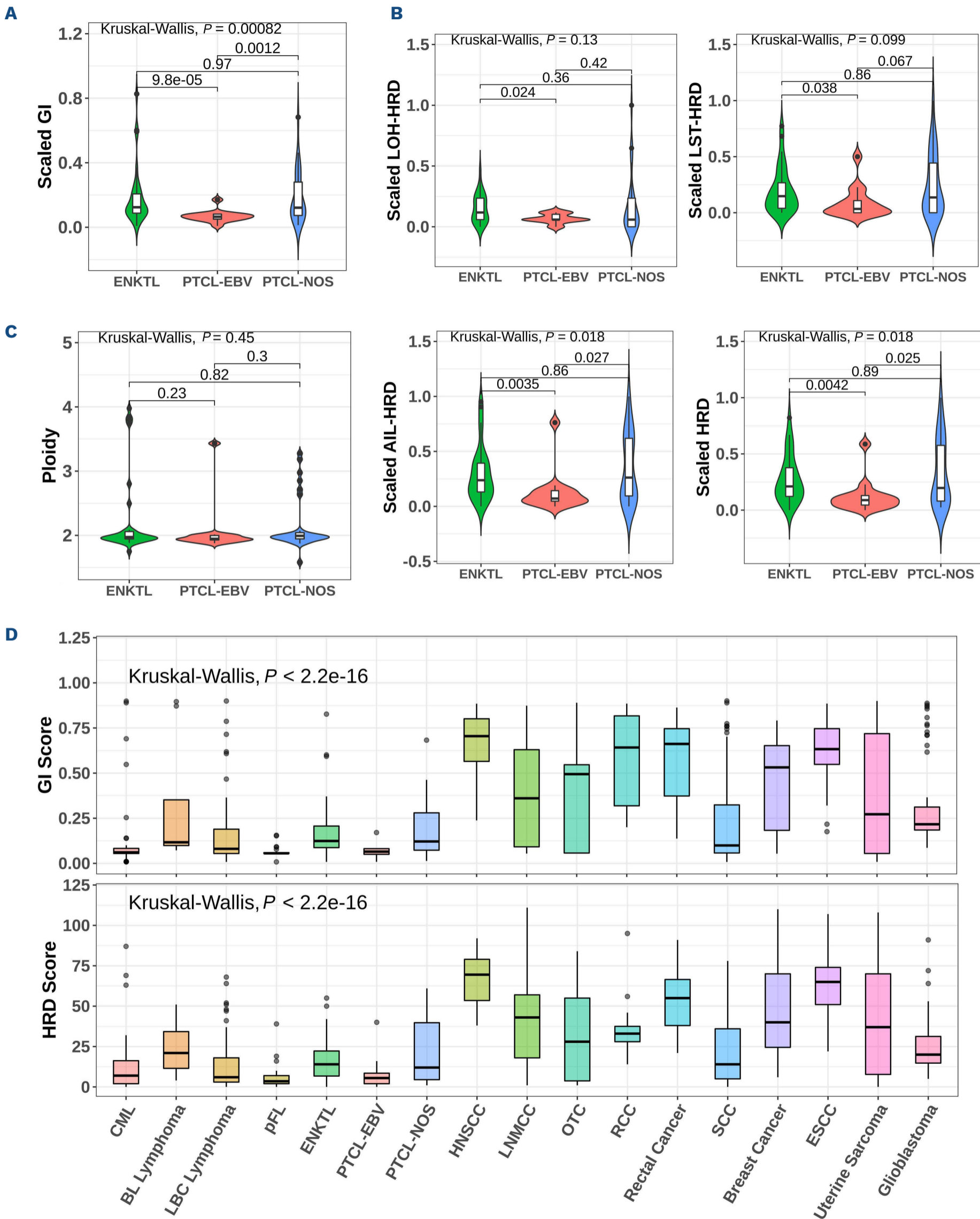
(Figure 2C, right panel). The sizes of gains and losses are known to vary across cancer types and these differences may be attributable to different mutagenic processes.¹⁷ Pairwise comparisons of copy number aberration size distributions indicated that all three diseases exhibited distinct patterns of gains and losses ($P < 0.05$, Kolmogorov-Smirnov test) (Figure 2D, E) with PTCL-EBV showing a propensity to smaller gains (~300 kb in size) and a unimodal distribution for losses peaking around 300 kb. To further examine the genomic complexities of the three disease groups, GI and HRD scores were calculated; the former based on the ratio of total length of regions with aberrant copy number and the latter on the loss of heterozygosity, telomere allelic imbalance and large-scale state transitions.¹¹ We observed that PTCL-EBV had significantly lower GI and HRD scores compared to ENKTL ($P < 0.001$ [GI], $P = 0.004$ [HRD], Mann-Whitney U) and PTCL-NOS ($P = 0.0012$ [GI], $P = 0.025$ [HRD]) (Figure 3A, B). Despite these lower scores, ploidy levels were similar across all three groups, indicating that these results were not attributable to differential rates of whole genome duplication (Figure 3C). The GI score remained significantly lower in PTCL-EBV T-lineage ($n = 13$) than in ENKTL T-lineage ($n = 9$) cases, indicating that the lower GI score in PTCL-EBV compared to ENKTL is not related to lineage. Nevertheless, future studies with larger sample sizes will be necessary for a comparison of lineage effects across the disease groups. In line with previous reports describing *TP53* alterations co-occurring with increased GI or HRD,¹⁸ we also observed that *TP53* losses were associated with higher GI score (Online Supplementary Figure S3) and were less frequent in PTCL-EBV (7.1%) than in ENKTL (26.5%; n.s., Fisher exact test) and PTCL-NOS (31.4%; $P = 0.03$) (Online Supplementary Table S5).

Using 14 publicly available Oncoscan datasets (Online Supplementary Table S7), we compared GI and HRD scores of other hematolymphoid neoplasms and solid cancers with those of PTCL-EBV, ENKTL and PTCL-NOS. Oncoscan datasets for T-cell lymphomas were unavailable. GI and HRD scores varied widely across cancer types, with the highest scores in solid cancers and the lowest in chronic myeloid

leukemia and pediatric-type follicular lymphoma (Figure 3D). Within hematolymphoid malignancies, high-grade lymphomas, such as Burkitt-like lymphomas, large B-cell lymphomas, ENKTL and PTCL-NOS, had higher GI than low-grade malignancies. Compared to other aggressive B-cell lymphomas, PTCL-EBV demonstrated a remarkably low GI score (all $P < 0.003$).

NF- κ B and immune pathways are overexpressed in PTCL-EBV

To explore the biological pathways associated with PTCL-EBV, we investigated genes that were differentially expressed between PTCL-EBV and ENKTL (EBVvsENKTL) or PTCL-NOS (EBVvsNOS). After filtering non-consensus coding sequence probes, 244 and 95 differentially expressed genes ($P < 0.01$, adjusted $P < 0.05$) were identified in EBVvsENKTL and EBVvsNOS, respectively (Online Supplementary Table S8). Interestingly, all 95 EBVvsNOS differentially expressed genes overlapped with the 244 from EBVvsENKTL. As expected, unsupervised hierarchical clustering of these 244 genes revealed three distinct clusters with PTCL-EBV separated from ENKTL and PTCL-NOS (Online Supplementary Figure S4). To assess differentially expressed genes for over-representation of gene ontology terms and protein-protein interactions, genes differentially expressed in EBVvsENKTL and EBVvsNOS were independently submitted to STRING.¹⁹ Both sets of differentially expressed genes were enriched for numerous immunity-related processes (Online Supplementary Tables S9 and S10) and known protein-protein interactions ($P < 0.005$) (Online Supplementary Figure S5). Subsequent analyses of known gene-gene interactions identified NF κ B-associated genes *BIRC3*, *NFKB1*, *TLR8* and *CD27* – which are upregulated in PTCL-EBV – as central nodes in the differentially expressed gene networks (Figure 4). To corroborate differential expression data at the protein level, multiplexed immunofluorescence was performed (Figure 5, Online Supplementary Figure S6A) and revealed significantly upregulated expression of *BIRC3* and p50 (*NFKB1*) in tumor (Online Supplementary Figure S6B, C) and non-tumor (Online Supplementary Figure S6E, F) cells of



Continued on following page.

Figure 3. Differences in genomic instability score, homologous recombination deficiency score and ploidy across different disease groups. Segmentation output data from OncoScan microarray (n=77 cases; ENKTL=34, PTCL-EBV=14, PTCL-NOS=29) was analyzed and quantified for scores of (A) GI, (B) LOH-HRD, LST-HRD, AIL-HRD and scaled HRD and (C) ploidy. (D) Comparison of GI- and HRD- scores across different cancer groups also profiled via OncoScan. Oncoscan datasets on T-cell lymphomas were unavailable. Wide variation of GI- and HRD- scores was observed across cancer types with HNSCC having highest scores while CML and pFL had lowest. High-grade lymphomas, such as Burkitt-like lymphomas, large B-cell lymphomas, ENKTL and PTCL-NOS had higher GI- and HRD-scores than low-grade lymphomas. Our results showed that PTCL-EBV exhibited significantly lower GI- and HRD- scores among aggressive lymphomas and various solid tumors. Statistical significance was determined using Kruskal-Wallis tests for differences among the three disease groups while Mann-Whitney U tests were used for pairwise comparisons. LOH: loss of heterozygosity; LST: large-scale state transitions; AIL: telomere allelic imbalance; BL: Burkitt-like; CML: chronic myeloid leukemia; ESCC: esophageal squamous cell carcinoma; HNSCC: head and neck squamous cell carcinoma; LBC: large B-cell; LNMCC: lymph node metastases in colon cancer; OTC: oral tongue carcinoma; pFL: pediatric-type follicular lymphoma; RCC: renal cell carcinoma; SCC: synchronous colorectal cancer; HRD: homologous recombination deficiency.

PTCL-EBV compared to ENKTL and PTCL-NOS. CD27 expression was significantly higher in tumor and non-tumor cells (*Online Supplementary Figure S6D, G*) of PTCL-EBV compared with ENKTL (both $P < 0.001$) but not with PTCL-NOS. Interestingly, the proportions of non-tumor cells which were double positive for CD27/BIRC3, CD27/p50, and triple positive for CD27/p50/BIRC3 within a single non-tumor cell, were also significantly higher in PTCL-EBV than in ENKTL and PTCL-NOS (*Online Supplementary Figure S6A, H-K*).

To further explore NF κ B across EBVs vs ENKTL and EBVs vs NOS, we performed gene set enrichment analysis using five curated sets of NF κ B target genes (*Online Supplementary Methods*). We observed consistent and significant upregulation of NF κ B target gene expression in PTCL-EBV compared to ENKTL and PTCL-NOS (Figure 6A). In addition, we found no significant difference in tumor content (*Online Supplementary Figure S7A*) and observed a rather homogeneous composition of the main immune components of the TME according to computational transcriptome deconvolution across the disease groups (*Online Supplementary Figure S7B*) using CIBERSORTx. This suggests that the upregulation of immune-related pathways in PTCL-EBV is unlikely to be related to tumor content or TME composition difference between the disease groups. Overall, these results indicate prominent immune pathway upregulation and NF κ B activation in PTCL-EBV, suggesting the potential role of persistent NF κ B signaling in the disease pathogenesis.

IFN γ , JAK-STAT and NF κ B is upregulation in PTCL-EBV and correlation with PD-L1

To further elucidate the biological pathways associated with GI, we correlated GI score to the expression of each gene across all samples, which resulted in a list of genes ranked by the Spearman rho. This list was submitted to gene set enrichment analysis to identify hallmark gene sets whose expression was associated with GI scores (*Online Supplementary Table S11*). Our top three gene sets – interferon_alpha_response (false discovery rate < 0.001), interferon_gamma_response (false discovery rate < 0.001)

and IL6_JAK_STAT3_signaling (false discovery rate = 0.001) (*Online Supplementary Figure S8A-C*) – displayed inverse correlations, indicating that these immune-related pathways are upregulated in PTCL-EBV and coincide with lower GI scores.

We previously reported that the expression of PD-L1 is higher in PTCL-EBV than in ENKTL.⁴ Given that both interferon_gamma_response (IFN γ) and STAT3 are able to induce PD-L1 expression at both gene and protein levels in cancers, including ENKTL,^{20,21} we correlated the gene expression of IFN γ and the IL6_JAK_STAT3 pathway with PD-L1 (*CD274*) to understand mechanisms driving PD-L1 upregulation in our disease groups. We observed a significant correlation between the gene expression of IFN γ ($R = 0.55$, $P < 0.001$) and IL6_JAK_STAT3 genes ($R = 0.79$, $P < 0.001$) with *CD274* (Figure 6B, C). Similarly, we also assessed the association between NF κ B activity and *CD274* since NF κ B can transcriptionally upregulate *CD274* expression.^{22,23} A significant correlation between the median expression of NF κ B transcriptional target genes and *CD274* was also observed ($R = 0.69$, $P < 0.001$) (Figure 6D). Overall, it is possible that the upregulation of PD-L1 in PTCL-EBV may be related to activation of IFN γ , IL6_JAK_STAT3 and NF κ B.

EBV miRNA are downregulated in PTCL-EBV compared to ENKTL

Since ENKTL and PTCL-EBV are both associated with EBV, we compared EBER expression, tumor content (via OncoScan), and EBV miRNA (via qPCR) in both diseases. There was no significant difference in EBER positivity (*Online Supplementary Figure S9A*) or tumor content (*Online Supplementary Figure S9B*) between the two diseases. Based on the gene expression of EBNA1, EBNA2, LMP1 and LMP2A by RT-PCR, the majority (9/13, 69%) of PTCL-EBV showed a type 2 EBV latency pattern, while four cases (31%) demonstrated a type 3 latency pattern (*Online Supplementary Table S12*). Interestingly, PTCL-EBV (n=9) displayed a widespread lower EBV miRNA expression compared to ENKTL (n=15) and clustered separately from it (*Online Supplementary Figure S10*). The expression of 32 of 42 (76%) EBV

miRNA was significantly lower in PTCL-EBV (adjusted $P < 0.05$, t -test) (Online Supplementary Table S13). To better understand the potential transcriptional impact of this differential miRNA regulation, we correlated the expression of each differentially expressed EBV miRNA and its predicted targets. Given that miRNA negatively regulate target mRNA,²⁴ all target genes that were negatively correlated (adjusted $P < 0.05$) to their corresponding EBV miRNA were analyzed ($n = 172$) (Online Supplementary Table S14). Strikingly, the pathways most

enriched (adjusted $P < 0.05$) within this set of genes represented either immunity or interferon signaling (Online Supplementary Table S15). After calculating a gene expression index (median expression) for these target genes, we observed significantly higher expression in PTCL-EBV ($P = 0.03$, Mann-Whitney U) (Online Supplementary Figure S11), which is consistent with lower EBV miRNA expression in this group. Overall, these results suggest that downregulation of EBV miRNA is unlikely to be related to a difference in tumor or EBER content and

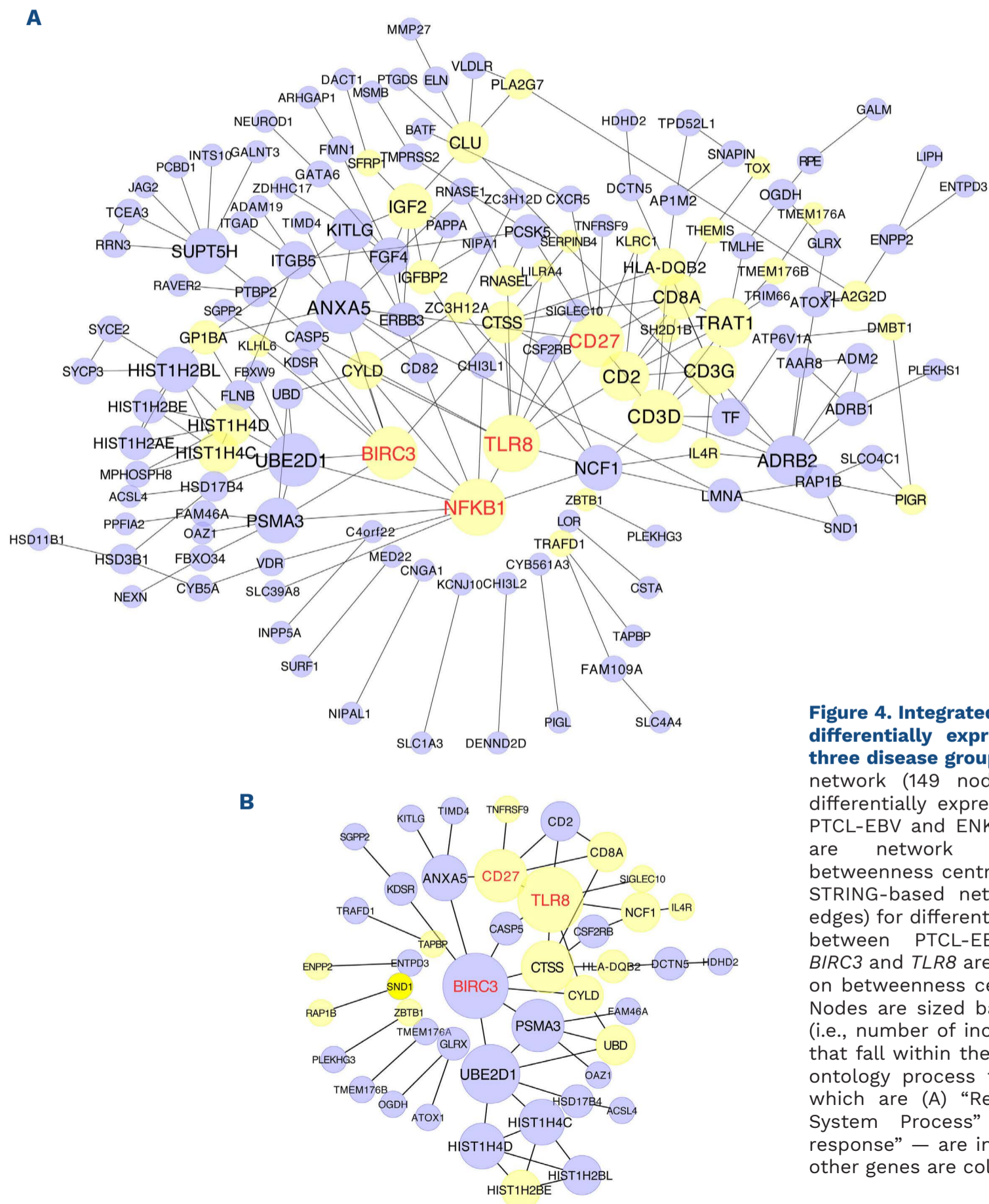


Figure 4. Integrated network analysis of differentially expressed genes in the three disease groups. (A) STRING-based network (149 nodes; 209 edges) for differentially expressed genes between PTCL-EBV and ENKTL. *NFKB1* and *TLR8* are network hubs based on betweenness centrality calculations. (B) STRING-based network (45 nodes; 52 edges) for differentially expressed genes between PTCL-EBV and PTCL-NOS. *BIRC3* and *TLR8* are network hubs based on betweenness centrality calculations. Nodes are sized based on their degree (i.e., number of incoming edges). Genes that fall within the most enriched gene ontology process for each network — which are (A) “Regulation of Immune System Process” and (B) “immune response” — are indicated in yellow. All other genes are colored light purple.

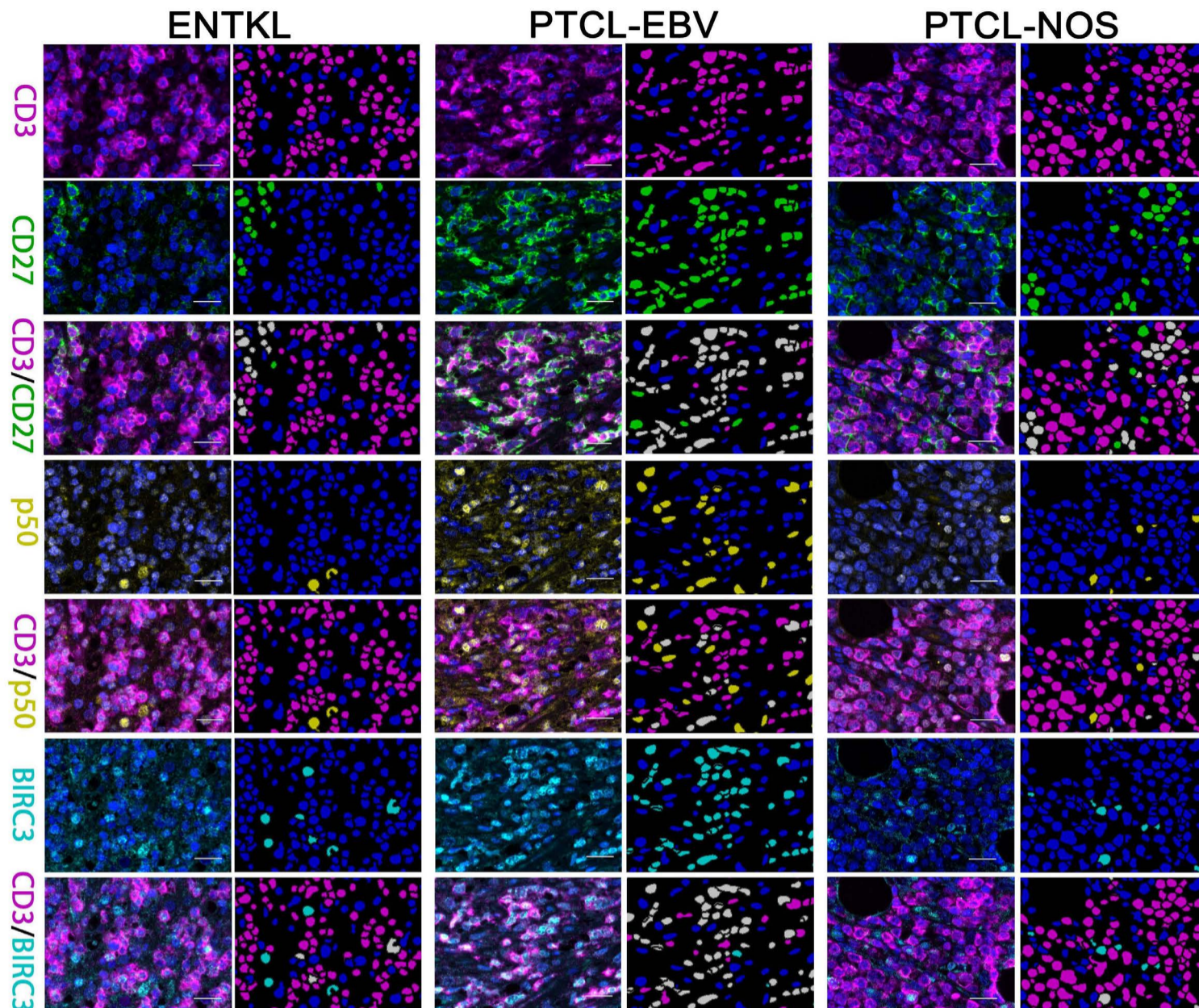


Figure 5. Multiplex immunofluorescence analysis of BIRC3, p50 (NFκB1) and CD27 across all three diseases. (A) Protein expression of CD27, p50 (NFκB1) and BIRC3 in ENKTL (left panel), PTCL-EBV (middle panel) and PTCL-NOS (right panel) using multiplexed immunofluorescence. For each panel, the left column represents the multiplexed immunofluorescence staining and the right column shows the corresponding multispectral analysis masks. PTCL-EBV showed higher expression of CD27 (membrane, green), p50 (NFκB1) (nuclear, yellow) and BIRC3 (nuclear, cyan), compared to ENKTL and PTCL-NOS. CD27⁺CD3⁺ cells are white while CD27⁺CD3⁻ are green in CD3/CD27 masks. P50⁺CD3⁺ cells are white while P50⁺CD3⁻ are yellow in CD3/p50 masks. BIRC3⁺CD3⁺ cells are white while BIRC3⁺CD3⁻ cells are cyan in CD3/BIRC3 masks. The scale bars indicate 100 μm.

could, in part, contribute to the distinctive pattern of immune gene transcription in PTCL-EBV.

PTCL-EBV showed frequent mutations of *TET2*, *PIK3CD* and *STAT3*

Based on the evidence that GI, gene expression, as well as EBV-miRNA patterns can delineate a distinct profile for PTCL-EBV, we further investigated whether this disease harbors mutations in known driver genes of PTCL-NOS, ENKTL and solid cancers using a 35-gene T/NK lymphoid panel and 484-gene NovoPMTM 2.0 assay (total 500 genes with 19 common genes covered in both panels).

The most commonly mutated gene was *TET2* (9/14, 64%) followed by *PIK3CD* (3/9, 33%), *STAT3* (3/16, 19%), *DDX3X* (2/10, 20%) and *PTPRD* (2/11, 18%) (*Online Supplementary Figure S12*). The variant allele frequency ranges for *TET2* in the NovoPMTM 2.0 panel and T/NK lymphoid panel were 22.2%-40.7% and 22%-76%, respectively. Given the tumor

purity of our samples and the high frequency of *TET2* mutations and their associated variant allele frequencies, it is unlikely that these mutations are attributable to clonal hematopoiesis of indeterminate potential (CHIP).²⁵ However, in the absence of blood samples from these patients, we cannot entirely rule out CHIP as a possible source of *TET2* mutation in some of our PTCL-EBV cases. Eight out of nine cases positive for *TET2* mutation were positive for CD8, indicating that they were not PTCL with T-follicular helper phenotype. Interestingly, TP53 mutations, commonly present in ENKTL, were not detected in our PTCL-EBV cases. The median number of mutations detected was 2.5 per sample (range, 1 to 11).

The tumor mutational burden score ranges from 0 to 7.86 mutations/MB (median 4.285 mutations/MB) (*Online Supplementary Figure S13A*). A tumor mutational burden of less than 5 is regarded as a low mutational burden in some studies.^{26,27} Eleven samples tested had a microsatel-

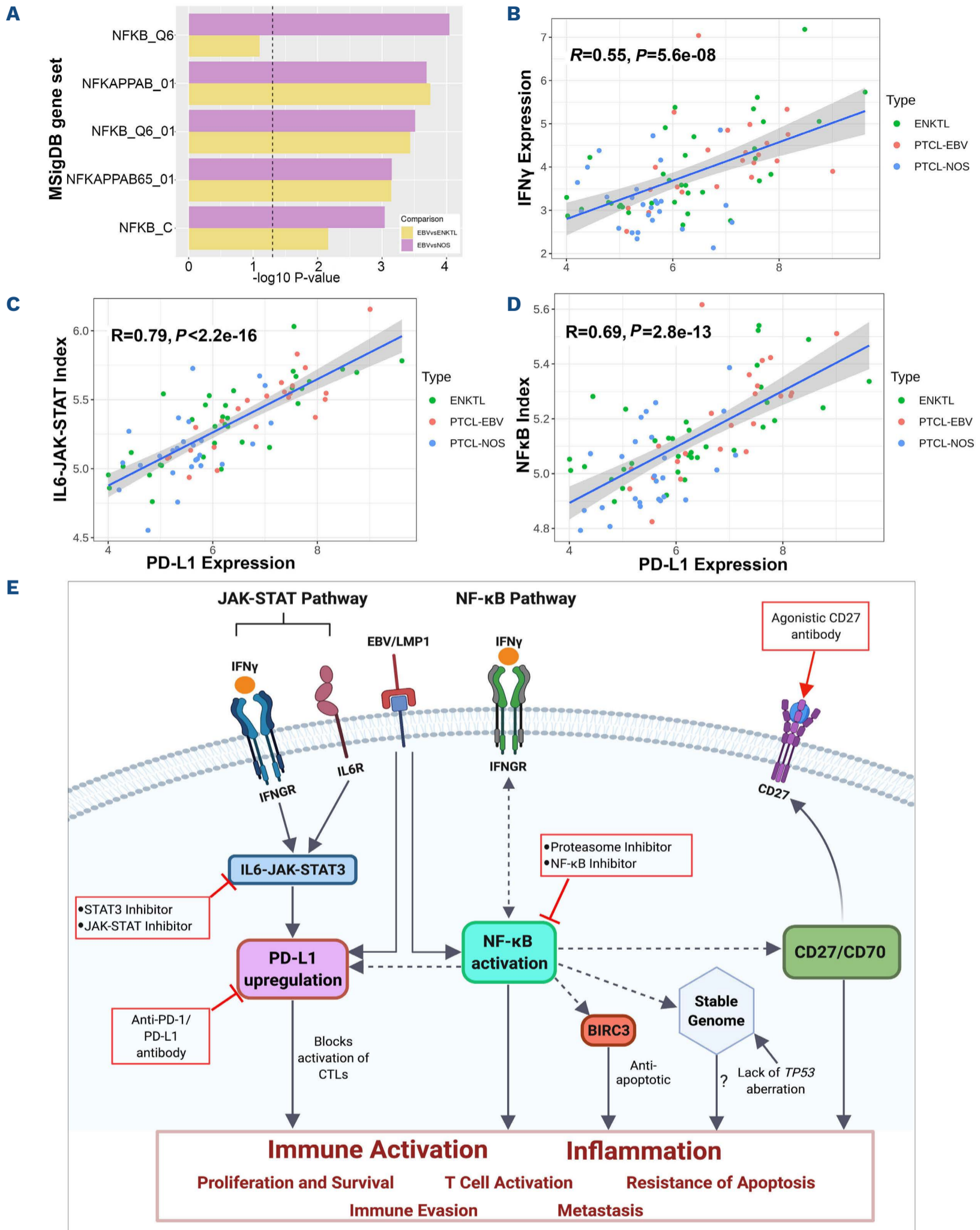


Figure 6. PTCL-EBV demonstrates NFκB transcriptional target gene upregulation and PD-L1 (CD274) expression associates with immune pathway activation across all three diseases. (A) Gene set enrichment analysis (GSEA) comparing PTCL-EBV to ENKTL (EBVvsENKTL) and PTCL-NOS (EBVvsNOS) across five sets of NFκB transcriptional target genes. Genes were ranked by their relative expression differences in EBVvsENKTL and EBVvsNOS then submitted to GSEA. All enrichment scores were positive indicating target gene upregulation in PTCL-EBV compared to ENKTL and PTCL-NOS. The vertical dashed line represents a 0.05 P value threshold. Correlation of PD-L1 (CD274) expression with (B) IFN γ , (C) the IL6_JAK_STAT pathway and (D) NFκB target gene expression across all three diseases. Our results showed that expression of IFN γ and IL6_JAK_STAT genes (median) correlated with PD-L1 gene expression. Taking the union of the five aforementioned gene sets, there was also a positive correlation between

Continued on following page.

NFκB transcriptional target gene expression (median) and PD-L1 expression. Correlations were assessed using the Spearman method. Rho and *P* values are shown. (E) Possible model of PTCL-EBV pathogenesis involving the activation of the NFκB pathway and upregulation of PD-L1, BIRC3, and CD27. BIRC3 plays key roles in the regulation of NFκB signaling and apoptosis. CD27 contributes to anti-tumor cytotoxic T-cell lymphocyte response in the host, T-cell exhaustion, compromise in antitumor immunity. In addition, EBV LMP1 and upregulation of IFNγ and IL6_JAK_STAT3 could also contribute to PDL1 overexpression in PTCL-EBV. Activation of these signaling pathways eventually contributes to inflammation, T-cell and immune activation, thereby promoting proliferation and survival, metastasis, immune evasion and oncogenesis. Some of these genes and signaling pathways may serve as potential therapeutic targets for PTCL-EBV and are indicated in red boxes. Dotted lines indicate hypothetical postulations which have not been experimentally validated in PTCL-EBV. Figure created with BioRender.com.

lite instability score below the threshold score of 0.4 (median 0.1882) and are regarded as being microsatellite stable (*Online Supplementary Figure S13B*).

PTCL-EBV is more aggressive and shows lower genomic instability than cytotoxic PTCL-NOS

Given that PTCL-EBV is characterized by a cytotoxic phenotype,^{2,5} we attempted to determine whether PTCL-EBV shows similarities with cytotoxic PTCL-NOS. We performed multivariate survival analysis and compared the GI and HRD scores, between PTCL-EBV, PTCL-NOS cytotoxic (n=15) and non-cytotoxic (n=11) cases. Interestingly, we observed that PTCL-EBV was significantly more aggressive than cytotoxic PTCL-NOS (HR=0.22, 95% CI: 0.08-0.58, *P*=0.002) but not non-cytotoxic PTCL-NOS (*Online Supplementary Table S16*).

PTCL-EBV exhibited significantly lower GI scores compared to both cytotoxic (*P*=0.041) and non-cytotoxic PTCL-NOS (*P*<0.001) (*Online Supplementary Figure S14*). HRD scores were lower in PTCL-EBV than in non-cytotoxic PTCL-NOS (*P*=0.021) but not cytotoxic PTCL-NOS. No significant difference was detected in survival, ploidy, and GI and HRD scores between cytotoxic and non-cytotoxic PTCL-NOS and there were no genes significantly differently expressed between the two. Overall, our results show a significant difference in overall survival and GI score between PTCL-EBV and cytotoxic PTCL-NOS, suggesting biological differences between these two tumors.

Discussion

PTCL-EBV is a rare and aggressive tumor that occurs mostly in East Asia. It is a poorly understood lymphoma that is not recognized yet as a distinct entity but is considered as a variant of PTCL-NOS in the current WHO classification.⁵ In line with published literature, all cases of PTCL-EBV in this study are from South-East/East Asia. Herein, we performed an integrative analysis to compare PTCL-EBV with ENKTL and PTCL-NOS, and our findings demonstrated distinctive features in PTCL-EBV which set it apart from the other two tumors. Our results support the consideration of PTCL-EBV as a distinct entity in the WHO classification.

Copy-number analysis of PTCL-EBV demonstrated a strik-

ing profile characterized by not only significantly fewer copy number aberrations, but also a different size distribution compared to ENKTL and PTCL-NOS. Remarkably, PTCL-EBV was more genomically stable than the other two diseases, as reflected by lower GI and HRD scores. High-grade lymphomas had higher GI and HRD scores than low-grade malignancies, compatible with reports documenting that GI is associated with aggressive lymphomas and high-grade transformation.^{28,29} Similarly, within and across a variety of solid tumors, increased copy number-based GI is associated with poor outcomes.³⁰ In this regard, the uniformly low GI and HRD scores in PTCL-EBV belies its aggressive behavior.

The discrepancy between low GI and aggressive behavior is novel but difficult to explain. Given the prominent immune-related gene expression profile, it is reasonable to hypothesize that the aggressiveness of PTCL-EBV may be related to a cancer-promoting inflammation which blocks anti-tumor immunity and directs the tumor microenvironment toward a tumor-permissive state.³¹ Interestingly, our findings showed that PTCL-EBV has few *TP53* mutations and has a paucity of *TP53* losses compared to ENKTL and PTCL-NOS. Given the paucity of *TP53* alterations in PTCL-EBV, it is possible that low GI in PTCL-EBV may be related to an unperturbed p53 tumor suppressor function, which is necessary to preserve genomic stability and integrity through cell-cycle arrest, senescence and apoptosis.³² Given that chromosome instability in diffuse large B-cell lymphomas can be suppressed by NFκB activation,³³ it is conceivable that NFκB activation in PTCL-EBV may also contribute towards the low GI but high aggressiveness of this tumor.^{34,35} Alternatively, there may be epigenetic deregulation driving oncogenesis in PTCL-EBV, which was not investigated in this study.³⁶

It is now known that cancer cells interact with surrounding stromal and immune cells to form a pro-tumorigenic inflammatory tumor microenvironment.³¹ Compared to ENKTL and PTCL-NOS, PTCL-EBV is characterized by striking activation of immune-related pathways, in particular, upregulation of NFκB and its associated genes, *BIRC3*, *NFKB1* and *CD27*, in both tumor and non-tumor cells. The upregulation of these three markers, either singly or co-localized with each other, suggests that there are different subsets of immune cells with varied combinations of *BIRC3*, p50 and *CD27* expression in PTCL-EBV, and that the

NF- κ B signaling pathway likely plays a role in promoting an active inflammatory tumor microenvironment in PTCL-EBV. NF κ B plays a key role in linking inflammation to cancer³¹ and targets different immune cells to modulate inflammation, tumorigenesis and metastasis.³⁷ The pronounced immune activation and NF κ B upregulation in PTCL-EBV may augment the local inflammatory state and suppress cytotoxic T-lymphocyte effector function, resulting in an immunosuppressive tumor microenvironment that enhances immune evasion and aggressive behavior.^{38,39} While CD27 normally activates NF κ B, promotes cell survival and enhances T- and B-cell receptor-mediated proliferative signals, dysregulation of CD27 signaling can result in T-cell exhaustion and dysfunction.^{40,41} Interestingly, we found that EBV-miRNA were predominantly downregulated in PTCL-EBV compared to ENKTL, which may further contribute to the inflammatory state with overexpression of immune-related genes.⁴² Based on our correlative data, we propose a model of PTCL-EBV pathogenesis involving NF κ B activation and upregulation of PD-L1, BIRC3 and CD27 (Figure 6E). Some of these pathways may serve as potential therapeutic targets for PTCL-EBV as drugs targeting JAK-STAT, NF κ B, STAT3, IFN γ , PD1/PD-L1 are either approved by FDA for different cancers or are being evaluated in clinical trials for lymphomas.⁴³⁻⁴⁵

The upregulation of the immune checkpoint protein PD-L1 in PTCL-EBV, inducible by IFN γ , may block the activation of the cytotoxic T-cell lymphocyte antitumor response, lead to T-cell exhaustion and promote immune evasion.^{23,46} In contrast to other lymphomas, this upregulation is unrelated to 9q24.1 gain.⁴⁷ Interestingly, we identified a significant correlation between the gene expression of PD-L1 and its known transcriptional-regulators: IFN γ , IL6_JAK_STAT3 and NF κ B. The overexpression of PD-L1 in PTCL-EBV, possibly a result of the upregulation of IFN γ , IL6_JAK_STAT3 and NF κ B pathways,^{20,23,37} suggests that targeting the PD-1/PD-L1 axis⁴³ may be a potentially effective therapeutic approach. Nevertheless, understanding the mechanisms causing PD-L1 upregulation, including structural variations in the 3' untranslated region of *PDL1*,⁴⁸ is essential for the design of more effective treatment strategies.²³

Our data demonstrate that the majority of PTCL-EBV cases show a type 2 EBV latency program,¹⁵ similar to that of ENKTL and other EBV-associated T/NK lymphoproliferative diseases.^{49,50} A minority revealed a type 3 latency pattern. It remains unclear whether this may reflect underlying immunosuppression as it is known that, in a subset of patients, PTCL-EBV is associated with autoimmune conditions, viral infections or diabetes mellitus which may impair the host's immune responses.^{1,51} The downregulation of EBV miRNA in PTCL-EBV compared to ENKTL suggests a difference in the EBV biology between the two diseases, although factors contributing to downregulation

of EBV miRNA have yet to be elucidated. Given that the predicted targets of the differentially expressed EBV miRNA are significantly enriched for immune-related pathways, it is tempting to postulate that the lower expression of EBV miRNA may contribute to the persistent expression of the many immune pathways in PTCL-EBV compared to ENKTL since miRNA are known to negatively regulate transcriptional gene expression.²⁴ Nevertheless, the complex interplay between EBV miRNA, viral and cellular target genes in EBV-associated T/NK-cell lymphomas requires further investigation.

In summary, PTCL-EBV is an aggressive lymphoma characterized by minimal GI, immune-related gene expression as well as activation of NF κ B and its associated genes. While further studies are needed to corroborate our proposed model, these findings highlight the importance of the crosstalk between tumor and microenvironment, provide new insights hinting at the disease pathogenesis and offer potential new therapeutic targets for this aggressive disease.

Disclosures

No conflicts of interest to disclose.

Contributions

CMMW and SC performed research, analyzed data and wrote the manuscript. TP, SML, WZ, LCYL, ADJ, W-JC and CT contributed to data interpretation and analysis. S-NC, C-KL and SF performed histological experiments. T-HC, KHKB, SG, SL, FZ and FI contributed to bioinformatics analysis. Y-HH, SK, SN, ET, Y-HK, JDK, S-SC, RKHA-Y, S-YT, S-TL, LMP, SDM and CKO selected cases and acquired data. LQM and FO performed the mutational analysis. JJP analyzed and interpreted data and wrote the manuscript. S-BN designed the project, analyzed data, and wrote and finalized the manuscript.

Acknowledgments

SBN is supported by the National Medical Research Council, Clinician Scientist Award, (CSAINV17nov016, WBS R-179-000-063-213), National Medical Research Council Open Fund Large Collaborative Grant, Singapore IYMP-Homa translational study (SYMPHONY) (NMRC OF-LCG18May-0028), and NUSMed Post-Doctoral Fellowship (PDF) (NUHSRO/2019/036/PDF/09). JJP is supported by the National Research Foundation Singapore and the Singapore Ministry of Education under its Research Centers of Excellence initiative. The computational work for this article was partially performed on resources of the National Supercomputing Center, Singapore (<https://www.nsc.sg>).

Data-sharing statement

De-identified data used in the preparation of this manuscript are available upon request.

References

- Ko YH, Chan JKC, Quintanilla-Martinez L. Virally associated T-cell and NK-cell neoplasms. In: Jaffe ES, Arber DA, Campo E, Harris NL, Quintanilla-Martinez L, editors. *Haematopathology*. Elsevier, Philadelphia 2017;565-598.
- Kato S, Asano N, Miyata-Takata T, et al. T-cell receptor (TCR) phenotype of nodal Epstein-Barr virus (EBV)-positive cytotoxic T-cell lymphoma (CTL): a clinicopathologic study of 39 cases. *Am J Surg Pathol*. 2015;39(4):462-471.
- Kato S, Takahashi E, Asano N, et al. Nodal cytotoxic molecule (CM)-positive Epstein-Barr virus (EBV)-associated peripheral T cell lymphoma (PTCL): a clinicopathological study of 26 cases. *Histopathology*. 2012;61(2):186-199.
- Ng SB, Chung TH, Kato S, et al. Epstein-Barr virus-associated primary nodal T/NK-cell lymphoma shows a distinct molecular signature and copy number changes. *Haematologica*. 2018;103(2):278-287.
- Pileri SA, Weisenburger DD, Sng I, et al. Peripheral T-cell lymphoma, NOS. In: Swerdlow SH, Campo E, Harris NL, et al., eds. *WHO Classification of Tumours of Haematopoietic and Lymphoid Tissues*. International Agency for Research on Cancer; Lyon. 2017:403-407.
- Pikor L, Thu K, Vucic E, Lam W. The detection and implication of genome instability in cancer. *Cancer Metastasis Rev*. 2013;32(3-4):341-352.
- Ahmad SS, Ahmed K, Venkitaraman AR. Science in focus: genomic instability and its implications for clinical cancer care. *Clin Oncol*. 2018;30(12):751-755.
- Oon ML, Lim JQ, Lee B, et al. T-cell lymphoma clonality by copy number variation analysis of T-cell receptor genes. *Cancers (Basel)*. 2021;13(2):340.
- Lee CS, Bhaduri A, Mah A, et al. Recurrent point mutations in the kinetochore gene KNSTRN in cutaneous squamous cell carcinoma. *Nat Genet*. 2014;46(10):1060-1062.
- Mermel CH, Schumacher SE, Hill B, Meyerson ML, Beroukhim R, Getz G. GISTIC2.0 facilitates sensitive and confident localization of the targets of focal somatic copy-number alteration in human cancers. *Genome Biol*. 2011;12(4):R41.
- Sinha S, Mitchell KA, Zingone A, et al. Higher prevalence of homologous recombination deficiency in tumors from African Americans versus European Americans. *Nat Cancer*. 2020;1(1):112-121.
- Cheadle C, Vawter MP, Freed WJ, Becker KG. Analysis of microarray data using Z score transformation. *J Mol Diagn*. 2003;5(2):73-81.
- Kato S, Yamashita D, Nakamura S. Nodal EBV⁺ cytotoxic T-cell lymphoma: a literature review based on the 2017 WHO classification. *J Clin Exp Hematop*. 2020;60(2):30-36.
- Ha SY, Sung J, Ju H, et al. Epstein-Barr virus-positive nodal peripheral T cell lymphomas: clinicopathologic and gene expression profiling study. *Pathol Res Pract*. 2013;209(7):448-454.
- Takahashi E, Asano N, Li C, et al. Nodal T/NK-cell lymphoma of nasal type: a clinicopathological study of six cases. *Histopathology*. 2008;52(5):585-596.
- Gong Q, Wang C, Zhang W, et al. Assessment of T-cell receptor repertoire and clonal expansion in peripheral T-cell lymphoma using RNA-seq data. *Sci Rep*. 2017;7(1):11301.
- Li Y, Roberts ND, Wala JA, et al. Patterns of somatic structural variation in human cancer genomes. *Nature*. 2020;578(7793):112-121.
- Pitt JJ, Riester M, Zheng Y, et al. Characterization of Nigerian breast cancer reveals prevalent homologous recombination deficiency and aggressive molecular features. *Nat Commun*. 2018;9(1):4181.
- Szklarczyk D, Gable AL, Lyon D, et al. STRING v11: protein-protein association networks with increased coverage, supporting functional discovery in genome-wide experimental datasets. *Nucleic Acids Res*. 2019;47(D1):D607-D613.
- Song TL, Nairismägi M-L, Laurensia Y, et al. Oncogenic activation of the STAT3 pathway drives PD-L1 expression in natural killer/T-cell lymphoma. *Blood*. 2018;132(11):1146-1158.
- Garcia-Diaz A, Shin DS, Moreno BH, et al. Interferon receptor signaling pathways regulating PD-L1 and PD-L2 expression. *Cell Rep*. 2017;19(6):1189-1201.
- Asgarova A, Asgarov K, Godet Y, et al. PD-L1 expression is regulated by both DNA methylation and NF- κ B during EMT signaling in non-small cell lung carcinoma. *Oncoimmunology*. 2018;7(5):e1423170.
- Shklovskaya E, Rizos H. Spatial and temporal changes in PD-L1 expression in cancer: the role of genetic drivers, tumor microenvironment and resistance to therapy. *Int J Mol Sci*. 2020;21(19):7139
- Ebert MS, Sharp PA. Roles for microRNAs in conferring robustness to biological processes. *Cell*. 2012;149(3):515-524.
- Ferrone CK, Blydt-Hansen M, Rauh MJ. Age-associated TET2 mutations: common drivers of myeloid dysfunction, cancer and cardiovascular disease. *Int J Mol Sci*. 2020;21(2):626
- Riviere P, Goodman AM, Okamura R, et al. High tumor mutational burden correlates with longer survival in immunotherapy-naïve patients with diverse cancers. *Mol Cancer Ther*. 2020;19(10):2139-2145.
- Liang WS, Vergilio J-A, Salhia B, et al. Comprehensive genomic profiling of Hodgkin lymphoma reveals recurrently mutated genes and increased mutation burden. *Oncologist*. 2019;24(2):219-228.
- Kamranvar SA, Gruhne B, Szeles A, Masucci MG. Epstein-Barr virus promotes genomic instability in Burkitt's lymphoma. *Oncogene*. 2007;26(35):5115-5123.
- Nagy M, Balázs M, Adám Z, et al. Genetic instability is associated with histological transformation of follicle center lymphoma. *Leukemia*. 2000;14(12):2142-2148.
- Hieronimus H, Murali R, Tin A, et al. Tumor copy number alteration burden is a pan-cancer prognostic factor associated with recurrence and death. *Elife*. 2018;7:e37294.
- Taniguchi K, Karin M. NF- κ B, inflammation, immunity and cancer: coming of age. *Nat Rev Immunol*. 2018;18(5):309-324.
- Yeo CQX, Alexander I, Lin Z, et al. p53 maintains genomic stability by preventing interference between transcription and replication. *Cell Rep*. 2016;15(1):132-146.
- Ramachandiran S, Adon A, Guo X, et al. Chromosome instability in diffuse large B cell lymphomas is suppressed by activation of the noncanonical NF- κ B pathway. *Int J Cancer*. 2015;136(10):2341-2351.
- Crawley CD, Kang S, Bernal GM, et al. S-phase-dependent p50/NF- κ B1 phosphorylation in response to ATR and replication stress acts to maintain genomic stability. *Cell Cycle*. 2015;14(4):566-576.
- Wang J, Jacob NK, Ladner KJ, et al. RelA/p65 functions to maintain cellular senescence by regulating genomic stability and DNA repair. *EMBO Rep*. 2009;10(11):1272-1278.
- Fennell KA, Bell CC, Dawson MA. Epigenetic therapies in acute myeloid leukemia: where to from here? *Blood*. 2019;134(22):1891-1901.
- Betzler AC, Theodoraki M-N, Schuler PJ, et al. NF- κ B and its role

- in checkpoint control. *Int J Mol Sci.* 2020;21(11):3949
38. Xia Y, Shen S, Verma IM. NF- κ B, an active player in human cancers. *Cancer Immunol Res.* 2014;2(9):823-830.
39. Lu C, Klement JD, Smith AD, et al. p50 suppresses cytotoxic T lymphocyte effector function to regulate tumor immune escape and response to immunotherapy. *J Immunother Cancer.* 2020;8(2):e001365.
40. Borst J, Hendriks J, Xiao Y. CD27 and CD70 in T cell and B cell activation. *Curr Opin Immunol.* 2005;17(3):275-281.
41. Riether C, Schürch C, Ochsenbein AF. Modulating CD27 signaling to treat cancer. *Oncoimmunology.* 2012;1(9):1604-1606.
42. Židovec Lepej S, Matulić M, Gršković P, Pavlica M, Radmanić L, Korać P. miRNAs: EBV mechanism for escaping host's immune response and supporting tumorigenesis. *Pathogens.* 2020;9(5.):353
43. Wang L, Qin W, Huo Y-J, et al. Advances in targeted therapy for malignant lymphoma. *Signal Transduct Target Ther.* 2020;5(1):15.
44. Godwin P, Baird AM, Heavey S, Barr MP, O'Byrne KJ, Gately K. Targeting nuclear factor-kappa B to overcome resistance to chemotherapy. *Front Oncol.* 2013;3:120.
45. Spaccarelli N, Rook AH. The use of interferons in the treatment of cutaneous T-cell lymphoma. *Dermatol Clin.* 2015;33(4):731-745.
46. Chihara N, Madi A, Kondo T, et al. Induction and transcriptional regulation of the co-inhibitory gene module in T cells. *Nature.* 2018;558(7710):454-459.
47. Green MR, Monti S, Rodig SJ, et al. Integrative analysis reveals selective 9p24.1 amplification, increased PD-1 ligand expression, and further induction via JAK2 in nodular sclerosing Hodgkin lymphoma and primary mediastinal large B-cell lymphoma. *Blood.* 2010;116(17):3268-3277.
48. Lim JQ, Huang D, Tang T, et al. Whole-genome sequencing identifies responders to pembrolizumab in relapse/refractory natural-killer/T cell lymphoma. *Leukemia.* 2020;34(12):3413-3419.
49. Xu ZG, Iwatsuki K, Oyama N, et al. The latency pattern of Epstein-Barr virus infection and viral IL-10 expression in cutaneous natural killer/T-cell lymphomas. *Br J Cancer.* 2001;84(7):920-925.
50. Chiang AK, Tao Q, Srivastava G, Ho FC. Nasal NK- and T-cell lymphomas share the same type of Epstein-Barr virus latency as nasopharyngeal carcinoma and Hodgkin's disease. *Int J Cancer.* 1996;68(3):285-290.
51. Yamashita D, Shimada K, Takata K, et al. Reappraisal of nodal Epstein-Barr virus-negative cytotoxic T-cell lymphoma: Identification of indolent CD5 diseases. *Cancer Sci.* 2018;109(8):2599-2610.